

Real-Time Implementation of STANAG 4539 High-Speed HF Modem

S. Saraç, F. Kara, C.Vural

Abstract—High-frequency (HF) communications have been used by military organizations for more than 90 years. The opportunity of very long range communications without the need for advanced equipment makes HF a convenient and inexpensive alternative of satellite communications. Besides the advantages, voice and data transmission over HF is a challenging task, because the HF channel generally suffers from Doppler shift and spread, multi-path, co-channel interference, and many other sources of noise. In constructing an HF data modem, all these effects must be taken into account. STANAG 4539 is a NATO standard for high-speed data transmission over HF. It allows data rates up to 12800 bps over an HF channel of 3 kHz. In this work, an efficient implementation of STANAG 4539 on a single Texas Instruments' TMS320C6747 DSP chip is described. The state-of-the-art algorithms used in the receiver and the efficiency of the implementation enables real-time high-speed data / digitized voice transmission over poor HF channels.

Keywords—High frequency, modem, STANAG 4539.

I. INTRODUCTION

THE HF band consists of the spectrum from 1.6 to 30 MHz. The importance of HF lies in the fact that in some circumstances, it allows very long range communications (several thousand kilometers). Unlike most other frequencies, which requires near line-of-sight (LOS) for proper operation, HF signals bounce back from the ionosphere, enabling beyond line-of-sight (BLOS) communications. The ionosphere is a region of electrically charged particles or gases in the atmosphere and it extends from approximately 50 to 600 kilometers above the earth's surface. This blanket of gases acts like a natural satellite, refracting the signal back to the earth several times depending on the amount of ionization before the signal reaches to its destination.

The HF signal generally propagates in two ways: ground waves and sky waves as shown in Fig. 1 [1]. Ground waves travel along the surface of the earth and consist of three components: surface waves, direct waves, and ground-reflected waves. Sky waves make long-range communications possible. Depending on the time of the day, atmospheric conditions, and operating frequency, radio waves are refracted, returning to earth hundreds or thousands kilometers away.

S. Saraç is with The Tubitak-Bilgem UEKAE (National Institute of Electronics and Cryptology), Gebze, Kocaeli, 41470, Turkey (phone: +90-262-648-1384; fax: +90-262-648-1100; e-mail: selim.sarac@uekae.tubitak.gov.tr).

F. Kara is with The Tubitak-Bilgem UEKAE (National Institute of Electronics and Cryptology), Gebze, Kocaeli, 41470, Turkey (phone: +90-262-648-1363; fax: +90-262-648-1100; e-mail: fkara@uekae.tubitak.gov.tr).

C. Vural is with the Department of Electrical and Electronics Engineering, Sakarya University, Sakarya, Turkey (e-mail: cvural@sakarya.edu.tr).

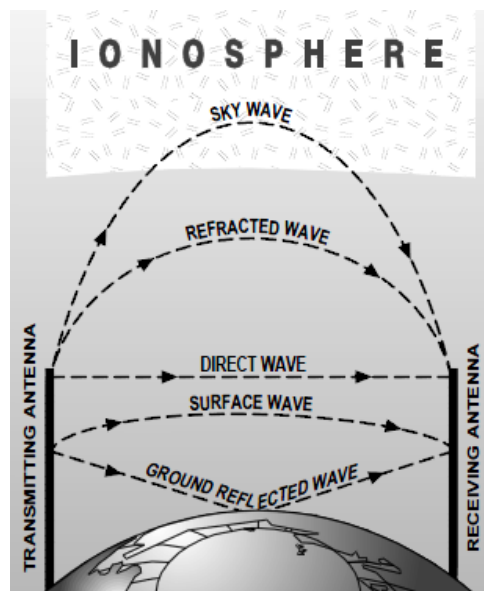


Fig. 1 HF channel propagation paths

Before 1960s, HF radio was the primary means of long-range communications for military applications. With the proliferation of satellite communications in 1960s and 1970s, HF technology saw a period of declining interest. Satellites transmitted data at higher speeds and eliminated the need for highly trained operators. However, with time, it became clear that satellites were vulnerable to physical damage and jamming, and it was expensive to build and maintain satellites and related infrastructure.

As a result, research and development in HF technology has intensified in the last two decades. Advances in LQA (Link Quality Analysis) and ALE (Automatic Link Establishment) led to dramatic improvements in link reliability and connectivity, eliminating the need for complex manual operating procedures. Hence, today HF is being recognized as a robust and highly competitive medium for long-haul communications.

A modem (modulator/demodulator) is a device or structure that converts bits (data or digitized voice) into audio to be sent by the radio transmitter, and converts audio received by the radio into bits. Current systems utilize the HF modem as a building block to provide a complete HF data system that includes adaptive data rate control, ARQ (automatic repeat request) protocols, ALE control, security architecture, and application protocols. A wide variety of applications are supported: secure voice, secure e-mail, position reporting / situational awareness, chat messaging, file transfer, and IP data over HF.

Besides all the advantages, HF channel has its own challenges and limitations. First of all, HF is a multipath fading channel, which means that a received signal may be

comprised of components arriving via multiple paths, adding constructively or destructively. These paths may include one or more sky waves and a ground wave. The arrival times of these components differ because of differences in path lengths. The multipath spread, which is defined as the maximum time difference between arriving signals, can be as high as several milliseconds for long-range HF communications. A modem receiver must employ adaptive equalization methods to mitigate the multipath spread.

Another challenge the HF channel presents is the Doppler shift or spread. Doppler shift is observed as a shift in carrier frequency when the transmitter or the receiver is moving. When combined with the multipath effect, the frequency shift turns into a frequency spread. Depending on the carrier frequency and the speed of the transmitter/receiver, the frequency shift can be as high as 75 Hz.

Other sources of noise in the HF channel include atmospheric noise (lightning and cosmic noise), man-made noise (electromagnetic interference by power lines, computer equipment, etc.), co-channel interference and intentional interference (jamming). A modem designer must take all these impairments into account.

There are several HF modem standards [2, 3, 4]. In this work, STANAG 4539 [2], a NATO standard that allows data rates up to 12800 bps on a 3 KHz HF channel, is implemented. STANAG 4539 is a recently developed standard which is commonly used as a physical layer block in modern HF tactical data systems. The implementation is done on Spectrum Digital's OVM-L137 development board [5], which incorporates a Texas Instruments' TMS320C6747 digital signal processor (DSP) chip [6]. The implementation includes modulation / demodulation, scrambler / descrambler, convolutional encoder / soft Viterbi decoder, interleaver / deinterleaver, signal detection, frame, symbol and carrier synchronization, adaptive channel estimation and equalization, Doppler estimation and correction, and end-of-message (EOM) detection. Simulation results show that the modem implementation satisfies performance constraints stated in the standard while enabling real-time high-speed HF data communications.

II. STANAG 4539

STANAG 4539 describes a family of serial-tone modem waveforms from 3200 to 12800 bps to ensure interoperability within complying HF radio networks. It refers to MIL-STD-188-110 Section 5.3 [3] for data rates between 150 and 2400 bps, and it refers to STANAG 4415 [4] for 75 bps very robust traffic waveform. The waveforms are self-identifying, which means that both the data rate and interleaver length settings are transmitted as a part of the waveform. This feature enables rapid adaptation of the modulation to changing channel conditions.

The modem waveform supports data rates of 3200, 4800, 6400, 8000 and 9600 bps. Uncoded operation at 12800 bps is also described. Modulation type depends on the data rate and is given in Table 1. For all data rates, the symbol rate is 2400 symbols-per-second and the carrier frequency is 1800 Hz. A single coding option, a constraint length 7, rate 1/2 convolutional code, punctured to rate 3/4, is used for all data rates.

To cope with block errors that often occur in the HF channel, a block interleaver is used to obtain 6 interleaver lengths ranging from 0.12 s to 8.64 s. Data is also scrambled prior to modulation in the transmitter in order to provide pseudo-randomness to the receiver for its carrier and symbol synchronization circuitry.

TABLE I
 MODULATION USED TO OBTAIN EACH DATA RATE

Data Rate (bps)	Modulation
3200	QPSK
4800	8PSK
6400	16QAM
8000	32QAM
9600	64QAM
12800	64QAM

The frame structure used in STANAG 4539 is shown in Fig. 2. An initial 287 symbol preamble is followed by 72 frames of alternating data and known symbols. Each data frame contains a data block consisting of 256 data symbols, followed by a 31-symbol mini-probe of known data. After 72 data frames (approximately 8.64 seconds), a 72 symbol subset of the initial preamble is reinserted to facilitate late acquisition and sync adjustment.

The synchronization preamble is used for synchronization, channel estimation and Doppler offset removal purposes. The first part consists of 184 random-like symbols, while the second part (final 103 symbols), which are common with the reinserted preamble, carries information regarding the data rate and interleaver settings. Mini-probes of length 31 are used both after each data frame and in the reinserted preamble for channel estimation and tracking, Doppler estimation and tracking and synchronization adjustment purposes. Using the 8PSK symbol mapping, each mini-probe is based on the repeated Frank-Heimiller sequence [7] because of its optimal properties for channel estimation and fast start-up synchronization. The standard also defines a 32-bit EOM sequence to be appended after the last input data bit of the message.

III. TRANSMITTER AND RECEIVER STRUCTURES

STANAG 4539 transmitter and receiver simplified software flow charts are given in Fig. 3 and Fig. 4, respectively.

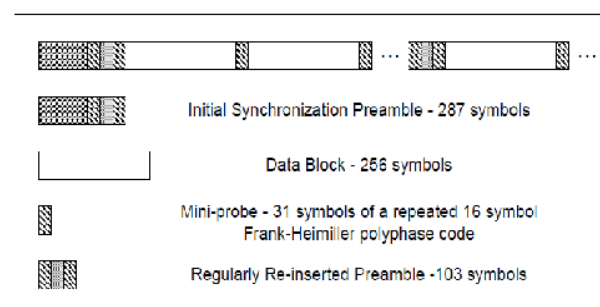


Fig. 2 Frame structure for all waveforms

Convolutional encoder, scrambler/ descrambler and interleaver/deinterleaver blocks are implemented as described in the standard [2]. A root-raised cosine filter is used as the pulse shaping filter in the transmitter and as the matched filter in the receiver.

The length of the filter is 20 symbols and the roll-off factor is 0.35. An upsampling rate of 4 is used in the transmitter, hence the sampling rate is 9600 Hz. Using a higher sampling rate in the receiver provides better symbol synchronization, so an oversampling rate of 8 is used, giving a sampling rate of 19200 Hz. Using even higher sampling rates is possible when enough processing power is provided.

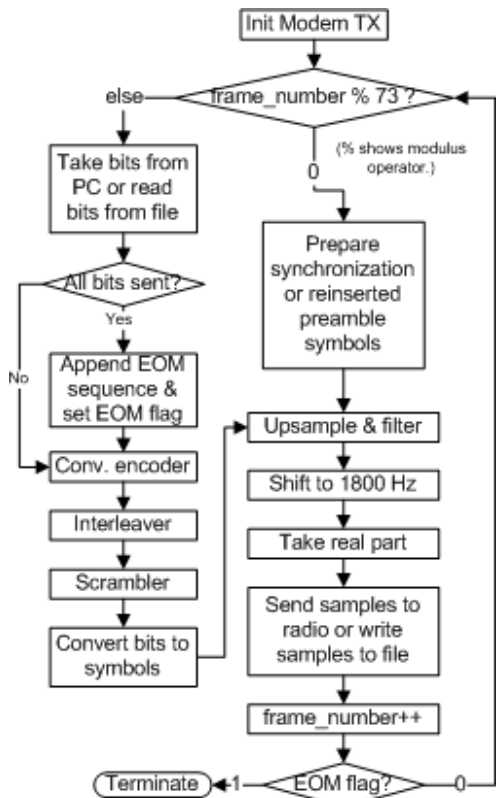


Fig. 3 Transmitter software flow chart

Shifting the signal to the carrier frequency (1800 Hz) is done by

$$y[n] = x[n] \exp(+j2\pi f_c n / f_s) \quad (1)$$

where $x[n]$ is the baseband signal, $y[n]$ is the shifted (modulated) signal, f_c is the carrier frequency, f_s is the sampling frequency, and n is the time index. The same formula is used in the receiver to shift the signal to baseband with the plus sign becoming a minus sign.

Hilbert Transform is used in the receiver to obtain an analytical signal (having only positive frequency components) from real-valued samples. The frequency response of the Hilbert Transform is given by [8].

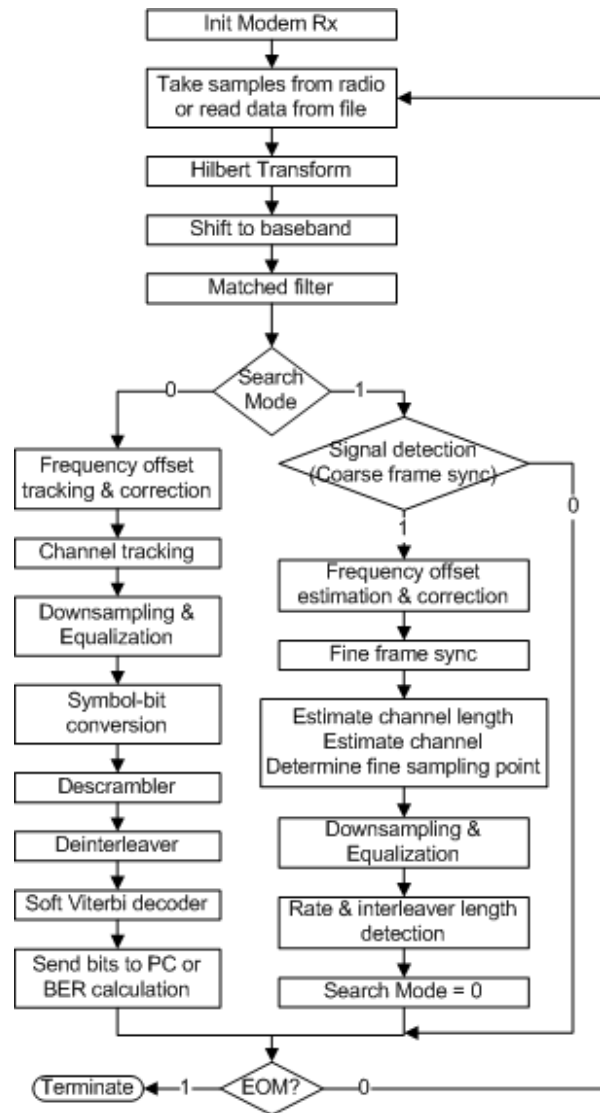


Fig. 4 Receiver software flow chart

$$H(f) = \begin{cases} -j, & f > 0 \\ 0, & f = 0 \\ +j, & f < 0 \end{cases} \quad (2)$$

Then, the analytical signal is obtained by

$$s_+[n] = s[n] + j \cdot s_h[n] \quad (3)$$

Where $s[n]$ is the real-valued signal, $s_h[n]$ is the Hilbert transform of $s[n]$, and $s_+[n]$ is the analytical signal. Ideally, Hilbert transform includes Fourier and inverse Fourier transforms, but because this is a time-consuming procedure, an FIR (finite-impulse response) filter approximation is used in the implementation.

For signal detection, a method that uses the delayed auto-correlation on the received signal [9] is used. Because the synchronization preamble (and the reinserted preamble) includes two similar 31-symbol miniprobes with a delay of 72

symbols, the delayed auto-correlation function gives a peak when the estimation window falls perfectly on the miniprobes. The following decision criterion is used:

$$\Psi[n] = \frac{\sum_{m=0}^{M-1} y[n+m] \cdot y^*[n+m+D]}{\sum_{m=0}^{M-1} (|y[n+m]|^2 + |y[n+m+D]|^2)} > T_h \quad (4)$$

In (4), $y[n]$ is the received and filtered baseband signal, M is the estimation length (31 symbols), D is the delay length (72 symbols), and T_h is a suitable threshold value. Starting from $n=0$, the search is continued until the threshold value is exceeded. In the noise-free case, the decision metric takes a maximum value of 1, but in practical cases, it reaches to a lower value. So, a threshold value of 0.8 is used. The time index of the maximum value also gives a rough frame synchronization point.

For frequency shift (Doppler) estimation, again the repeating miniprobe patterns are utilized. In the time domain, frequency shift manifests itself as a shift in the phase, i.e. $x_s(t) = x(t)\exp(2\pi j f_o t)$, where $x(t)$ and $x_s(t)$ are the original and frequency-shifted signals, respectively, f_o is the frequency offset, and t is time (in the continuous case). Let $S = |S| \exp(j\varphi)$ be a mini-probe symbol sent at time $t = t_o$. The same miniprobe symbol is sent again at $t = t_o + \Delta t$, where Δt is 72 symbols. Let S_1 and S_2 be two received miniprobe symbols that have a time distance of 72 symbols. They are expressed by

$$\begin{aligned} S_1 &= |S_1| \exp(j\varphi) \exp(2\pi j f_o t_o) = |S_1| \exp[j(\varphi + 2\pi f_o t_o)] \\ S_2 &= |S_2| \exp(j\varphi) \exp(2\pi j f_o (t_o + \Delta t)) \\ &= |S_2| \exp[j(\varphi + 2\pi f_o (t_o + \Delta t))] \end{aligned} \quad (5)$$

If we calculate the phase difference as

$$\Delta\varphi = (\varphi + 2\pi f_o (t_o + \Delta t)) - (\varphi + 2\pi f_o t_o) = 2\pi f_o \Delta t \quad (6)$$

then the frequency shift can be calculated as

$$f_o = \Delta\varphi / (2\pi\Delta t). \quad (7)$$

In the discrete-time domain, this relationship can be expressed as

$$f_o = \Delta\varphi / (2\pi D / f_s) \quad (8)$$

Where D is the distance between symbols and f_s is the sampling rate. With this method, there is an upper bound for frequency shift estimation, because the phase difference is limited and it can be between $-\pi$ and π . Hence, the maximum detectable frequency offset is

$$f_o = (\pm\pi) / (2\pi D / f_s) = \pm f_s / (2D). \quad (9)$$

The frequency shift estimation process is done by using multiple pairs of symbols (in which the distances between the pairs are the same) to provide robustness to noise. Frequency offset tracking is done with the same method by using the mini-probe symbols surrounding the data frames. After f_o is estimated, frequency shift correction is applied on the signal as $x[n] = x_s[n] \exp(-2\pi j f_o n / f_s)$.

Fine frame synchronization is achieved by cross-correlating the received signal with the mini-probe symbols by the following formula:

$$n_f = \arg \max_n \left(\sum_{m=0}^{M-1} y[n+m] S_m^* \right) \quad (10)$$

Where S_m is the m -th mini-probe symbol and n_f is the fine frame synchronization point. n covers the range from $n_0 - b_1$ to $n_0 + b_1$, where n_0 is the coarse frame synchronization point and b_1 is a suitable backup value.

Symbol synchronization (determining fine sampling point) is done in conjunction with channel estimation by using the mini-probe symbols again. Least-squares channel impulse response estimation for some arbitrary sampling point n is given by

$$\hat{\mathbf{h}}_n = (\mathbf{B}^H \mathbf{B})^{-1} \mathbf{B}^H \mathbf{y}_n \quad (11)$$

where \mathbf{B} is a $M-L+1 \times L$ convolution matrix whose rows correspond to different shifts of the transmitted sequence of mini-probe symbols, M is the number of mini-probe symbols, L is the number of taps, \mathbf{y}_n is the $M-L+1 \times 1$ received symbol sequence vector starting from n , and H denotes Hermitian transpose. The error corresponding to sampling point n is given by

$$e_n = \|\mathbf{B} \cdot \hat{\mathbf{h}}_n - \mathbf{y}_n\|_2 \quad (12)$$

where $\|\cdot\|_2$ denotes the $L-2$ norm. The fine sampling point can be calculated as

$$n_s = \arg \min_n (e_n) \quad (13)$$

where n covers the range from $n_f - b_2$ to $n_f + b_2$, n_f is the fine frame synchronization point and b_2 is another suitable backup value. The channel impulse response then becomes the least-squares channel estimation at point n_s . Channel tracking is implemented by estimating the channel for each mini-probe sequence and interpolating it along the data symbols. Decision-feedback equalization (DFE) [9] is used to reverse the channel effect on the received data.

The receiver software halts active reception when the 32-bit EOM sequence is detected or when there is a sudden and permanent drop in the received signal power.

IV. DSP IMPLEMENTATION

The implementation is done using the standard C language on Spectrum Digital's OVM-L137 development board. The OMAP-L137 EVM is a standalone development platform that enables users to evaluate and develop applications for the OMAP-L137 processor, which consists of a 456 MHz C6747 DSP floating point processor and a 300 MHz ARM926EJ-S processor. It has USB, ethernet and RS-232 interfaces to communicate with the PC, an AIC (analog interface circuit, A/D and D/A converters) to interface with the radio, and 64 Megabytes of SDRAM on board. Schematics and application notes are available to ease hardware development and reduce product development time.

Texas Instruments' TMS320C6747 DSP chip (456 MHz) is a low-power applications processor based on fixed/floating point C674x DSP core. It consumes significantly lower power than other members of DSP families. It is primarily used in applications such as industrial control, professional audio and portable audio/video/communication devices. It has 320 kilobytes of on-chip RAM, an enhanced direct-memory-access controller, two external memory interfaces, three configurable 16550 type UART modules, an LCD controller, two serial peripheral interfaces (SPI), multimedia card (MMC)/ secure digital (SD), two master/slave inter-integrated circuit controllers, one host-port interface (HPI), and USB 1.1 OHCI (host) with integrated PHY (USB1).

For effective utilization of the DSP, some modifications to the standard C implementation are done. These are:

1- DSP library object codes [10] are used whenever possible. The library is provided by the manufacturer and it contains C-callable assembly-optimized general-purpose signal processing routines. By using these routines, execution speeds considerable faster than equivalent code written in standard ANSI C language are achieved. The following functions are implemented using DSP library:

- Trigonometric functions
- FIR filtering
- Auto-correlation and cross-correlation
- Matrix multiplication and inversion
- Vector multiplication
- Soft Viterbi decoding

2- For some arithmetic and data conversion operations, C/C++ intrinsics [11] are used instead of C/C++ standard runtime operations. Intrinsics are used just as function calls and allow the programmer to express the meaning of certain assembly statements that would otherwise be cumbersome or inexpressible in C/C++, enabling more efficient utilization of the DSP.

3- High-level optimization option of the compiler is invoked. This option performs software pipelining, loop optimizations, loop unrolling, register optimization, reordering function declarations, and many other optimization techniques automatically.

V. SIMULATION RESULTS

Performance of the high data rate modem is tested using a baseband HF simulator patterned after the Watterson model in

accordance with ITU-R 520-1 [12]. Bit error rate (BER) performance is measured with the channel simulator programmed to simulate the following channels:

- The AWGN (additive white Gaussian noise) consists of a single, non-fading path.
- The Rician channel consists of two independent but equal average power paths, with a fixed 2 ms delay between paths. The first path is non-fading. The second path is a Rayleigh fading path with a fading bandwidth of 2 Hz.
- The ITU-R Poor channel consists of two independent but equal average power Rayleigh fading paths, with a fixed 2 ms delay between paths, and with a fading bandwidth of 1 Hz.

For each data rate and channel type, the SNR (signal-to-noise ratio) is investigated in which a coded BER of 10^{-4} is achieved using fixed-frequency operation and employing the maximum interleaving period (the 72-frame "very long" interleaver). The results are given in Table 2. In the table, the first value is the SNR that should be satisfied according to the standard, and the second value is the SNR that our implementation operates at. It can be seen that in most of the cases, our implementation achieves the coded BER of 10^{-4} at lower SNR values than that are recommended in the standard.

The details of one of the simulations are given below. Data rate is 4800 bps, interleaver length is 72 frames and the poor channel is simulated with a frequency offset of 50 Hz and SNR of 22 dB. The gains of the first and the second paths are given in Fig. 5. The equalizer experiences no problem in decoding the data when both of the paths do not experience fading or just one of the paths is exposed to a deep fade. But as seen in the figure, both the first and the second paths incur fading simultaneously at about 6.5-th and 8.5-th seconds, and the equalizer fails to decode the symbols correctly.

This phenomenon can be observed in Fig. 6, where the error magnitudes are plotted with respect to time (frame number) and symbol index.

TABLE II
 MODEM PERFORMANCE REQUIREMENTS AND IMPLEMENTATION RESULTS

User data rate (bps)	Average SNR (dB) for BER not to exceed 10^{-4}		
	AWGN Channel	Rician Channel	Poor Channel
12800	27 / 22	-	-
9600	21 / 18	30 / 29	30 / 29
8000	19 / 16	25 / 25	26 / 26
6400	16 / 14	21 / 21	23 / 22
4800	13 / 8	17 / 15	20 / 20
3200	9 / 7	12 / 12	14 / 14

At frames about 50 and 70, which correspond to 6.5-th and 8.5-th seconds, the amount of error is too much. As a result, the constellation diagram is scattered as shown in Fig. 7 and the bits are extracted erroneously at those frames. But, because the very long interleaver option is used, the soft Viterbi decoder experiences no difficulty in correcting the erroneous

bits that are not no longer together but scattered throughout the data. Hence zero BER is achieved.

decoder-aided (turbo) equalization methods can be studied to improve the performance and to further decrease the processor cycle requirements.

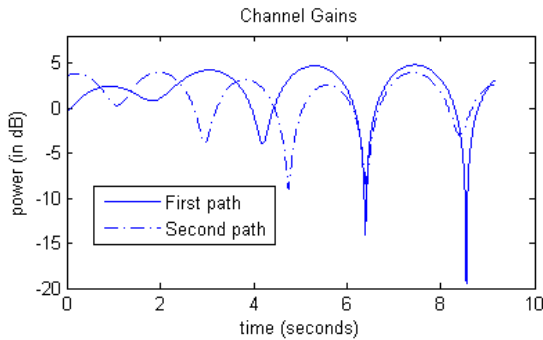


Fig. 5 Channel gains for the first and second paths

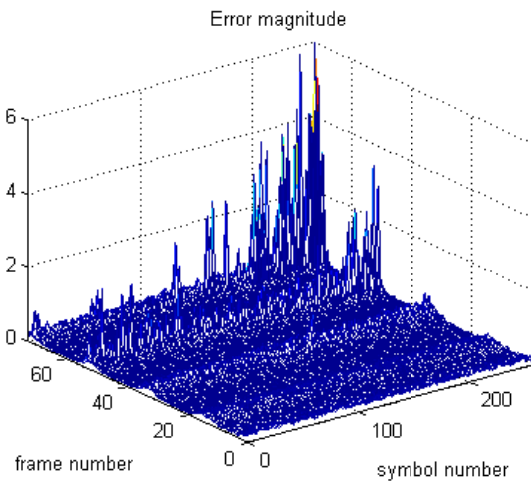


Fig. 6 Error magnitude

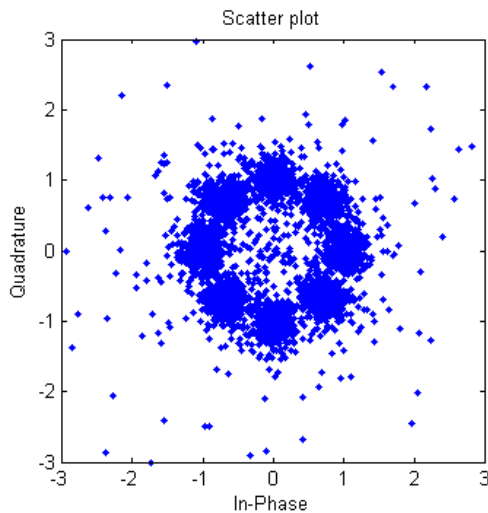


Fig. 7 Constellation diagram of the received symbols

VI. CONCLUSION

In this work, STANAG 4539 high-speed HF modem is implemented to work real-time on a Texas Instruments' DSP chip. Real-time operation is achieved by applying optimization methods that are specific to the DSP used. Simulation results show that the performance constraints that are stated in the standard are met. As a future work, iterative

REFERENCES

- [1] "Radio Communications in the Digital Age, Volume 1: HF Technology (Edition 2)", Harris Corporation, 2005.
- [2] STANAG 4539, "Technical Standards for Non-Hopping HF Communications Waveforms", NATO, 2005.
- [3] MIL-STD-188-110B, "Military Standard - Interoperability and Performance Standards for Data Modems", US Dept. of Defence, 2000.
- [4] STANAG 4415, "Characteristics of a Robust Non-Hopping Serial Tone Modulator/Demodulator for Severely Degraded HF Radio Links", NATO, 1997.
- [5] "OMAP-L137 Evaluation Module Technical Reference", Spectrum Digital, Inc., 2008.
- [6] SPRS377D, "TMS320C6745, TMS320C6747 Fixed-Floating-Point Digital Signal Processor Datasheet", Texas Instruments, 2010.
- [7] R. C. Heimiller, "Phase Shift Pulse Codes with Good Periodic Correlation Properties", IRE Trans. Info. Theory IT-6, pp. 254-257, Oct. 1961.
- [8] J. Proakis, "Digital Communications", McGraw Hill, 4th Edition, 2000.
- [9] H. Meyr, M. Moeneclaey, S. A. Fechtel, "Digital Communication Receivers, Synchronization, Channel Estimation, and Signal Processing", Wiley-Interscience, 1997.
- [10] SPRU657C, "TMS320C67x DSP Library Programmer's Reference Guide", Texas Instruments, 2008.
- [11] SPRU187Q, "TMS320C6000 Optimizing Compiler", Texas Instruments, 2010.
- [12] ITU, "Recommendation 520-1 Use of High Frequency Ionospheric Channel Simulators", Recommendations and Reports of the CCIR, Vol. III, pp. 57-58, Geneva.